J Neurophysiol 124: 1469–1479, 2020.
First published September 23, 2020; doi:10.1152/jn.00338.2020.

RESEARCH ARTICLE | *Spinal Networks and Spinal Cord Injury: A Tribute to Reggie Edgerton*

Redundancy and multifunctionality among spinal locomotor networks

Bau N. Pham,[1] Jiangyuan Luo,[2] Harnadar Anand,[3] Olivia Kola,[2] Pia Salcedo,[4] Connie Nguyen,[5] Sarah Gaunt,[6] Hui Zhong,[7] Alan Garfinkel,[7] Niranjala Tillakaratne,[7,8] and V. Reggie Edgerton[7,8,9,10,11,12]

[1]*Department of Bioengineering, University of California, Los Angeles, California;* [2]*Department of Neuroscience, University of California, Los Angeles, California;* [3]*Institute for Society and Genetics, University of California, Los Angeles, California;* [4]*Department of Psychobiology, University of California, Los Angeles, California;* [5]*Department of Ecology and Evolutionary Biology, University of California, Los Angeles, California;* [6]*Department of Molecular Cellular and Developmental Biology, University of California, Los Angeles, California;* [7]*Department of Integrative Biology and Physiology, University of California, Los Angeles, California;* [8]*Brain Research Institute, University of California, Los Angeles, California;* [9]*Department of Neurobiology, University of California, Los Angeles, California;* [10]*Department of Neurosurgery, University of California, Los Angeles, California;* [11]*Institut Guttmann, Hospital de Neurorehabilitació, Universitat Autònoma de Barcelona, Badalona, Spain; and* [12]*Centre for Neuroscience and Regenerative Medicine, Faculty of Science, University of Technology Sydney, Ultimo, Australia*

Submitted 10 June 2020; accepted in final form 13 September 2020

Pham BN, Luo J, Anand H, Kola O, Salcedo P, Nguyen C, Gaunt S, Zhong H, Garfinkel A, Tillakaratne N, Edgerton VR. Redundancy and multifunctionality among spinal locomotor networks. *J Neurophysiol* 124: 1469–1479, 2020. First published September 23, 2020; doi:10.1152/jn.00338.2020.—c-Fos is used to identify system-wide neural activation with cellular resolution in vivo. However, c-Fos can only capture neural activation of one event. Targeted recombination in active populations (TRAP) allows the capture of two different c-Fos activation patterns in the same animal. So far, TRAP has only been used to examine brain circuits. This study uses TRAP to investigate spinal circuit activation during resting and stepping, giving novel insights of network activation during these events. The level of colabeled (c-Fos+ and TRAP+) neurons observed after performing two bouts of stepping suggests that there is a probabilistic-like phenomenon that can recruit many combinations of neural populations (synapses) when repetitively generating many step cycles. Between two 30-min bouts of stepping, each consisting of thousands of steps, only ~20% of the neurons activated from the first bout of stepping were also activated by the second bout. We also show colabeling of interneurons that have been active during stepping and resting. The use of the FosTRAP methodology in the spinal cord provides a new tool to compare the engagement of different populations of spinal interneurons in vivo under different motor tasks or under different conditions.

NEW & NOTEWORTHY The results are consistent with there being an extensive amount of redundancy among spinal locomotor circuits. Using the newly developed FosTRAP mouse model, only ~20% of neurons that were active (labeled by *Fos*-linked tdTomato expression) during a first bout of 30-min stepping were also labeled for c-Fos during a second bout of stepping. This finding suggests variability of neural networks that enables selection of many combinations of neurons (synapses) when generating each step cycle.

Correspondence: B. N. Pham (bphamjr@gmail.com); V. Reggie Edgerton (vre@ucla.edu).

c-Fos; FosTRAP; multifunctionality; redundancy; spinal cord

INTRODUCTION

Locomotion is a complex behavior that is modulated by a variety of highly integrated and interdependent neural networks throughout the nervous system. These movements can be executed repetitively under highly variable conditions and adversity. How does the central nervous system reduce an almost infinite movement space with a finite network of neurons to perform a task with a critical level of accuracy in a continuously changing environment?

Previous research has suggested that the nervous system can reduce the dimensionality of actionable neural control elements by having a modular structure (Caggiano et al. 2016; Cheung et al. 2005; Ivanenko et al. 2013; Saltiel et al. 2005) and having multifunctional interneurons (Berkowitz 2010; Berkowitz et al. 2010; Borowska et al. 2013; Briggman and Kristan 2008; Esposito et al. 2014; Hao and Berkowitz 2017; Jankowska 2001; Levine et al. 2014). The concept of modularity breaks down all actionable movement into "motor primitives," a set of elementary building blocks that coordinate groups of muscles (Caggiano et al. 2016; Ivanenko et al. 2013). These motor primitives can then be variably recombined to generate a wide range of complex movements. Examples of this have been shown using optogenetic stimulation in which activation of a neuron elicits motor activity in a group of muscles (Caggiano et al. 2016; Levine et al. 2014). Electrophysiological recordings have demonstrated the activity of single neurons that are active during different types of locomotor behavior (Berkowitz 2010; Berkowitz et al. 2010; Hao and Berkowitz 2017), thus showing the multifunctionality (Briggman and Kristan 2008) of these motor primitives. This modularity and multifunctionality can

result in redundancy in which many combinations of neurons and neuronal networks can generate the same task (Li et al. 2016; Loy et al. 2002; Shenoy et al. 2013; So et al. 2012). A feature of redundancy is the variability that is found in all movements, even in highly repetitive tasks, such as stepping. This variability can be found in repeating movements (Haar et al. 2017; Sauerbrei et al. 2015) and processing sensory stimuli (Benedetti et al. 2009; Lisberger and Medina 2015). Variability exists at many different levels of the nervous system ranging from synapses and single cells (Benedetti et al. 2009; Sauerbrei et al. 2015) to population activity (Haar et al. 2017). Most of these studies have focused on the brain, but few studies have considered the degree to which spinal networks contribute to the neural variability when performing a motor task. Some suggest that this variability reflects inefficiencies in motor networks. However, it could provide a robust means for the nervous system to execute a wide array of tasks under many circumstances (Ivanenko et al. 2013; Latash 2012a, 2012b).

The above studies have demonstrated neural variability and the multifunctional nature of spinal interneurons using electrophysiological and optical techniques that have single-cell resolution. These techniques are volumetrically constrained and have limitations when studying system-level networks that span the entire central nervous system. Techniques like functional magnetic resonance imaging (fMRI) and c-Fos labeling can show neural activation that spans entire networks and systems. However, fMRI does not have cellular resolution. Although c-Fos has cellular resolution, it has not been feasible, until recently, to use it to measure activity in more than one event in the same animal.

The recent emergence of targeted recombination in active populations (TRAP) mice provides a new tool and methodology that can study the concept of neuronal network redundancy in the spinal cord. This model allows for the comparison of two c-fos-like activation patterns due to two different or even the same tasks in the same animal, where the first event is "TRAPed" by tdTomato and the second event is captured by normal c-Fos labeling. To date, the FosTRAP mouse model has been used primarily to study neural networks in the brain. The present study aims to determine whether we can capitalize on TRAP mice to study the uniqueness or the level of shared function of spinal networks in the same or different motor tasks.

In this study, the use of colabeling (tdTomato+ and c-Fos+) has shown shared components in the execution of two different tasks (stepping and resting) and suggests redundancy when repeating bouts of stepping at the same speed and duration. The ability to colabel active cells after performing the same motor event provides an opportunity to estimate the different combinations of neurons that can execute a highly repetitive task such as stepping. Although many studies have provided some insight into the level of redundancy when repeating a sensorimotor task, no previous experimental methodologies, to our knowledge, have provided a strategy to directly estimate redundancy at a system-wide level. In addition, the FosTRAP model provides a novel tool to study in vivo spinal physiology under different experimental conditions and applications.

MATERIALS AND METHODS

Animals. These experiments used an adult FosTRAP mouse line developed at Stanford by the Luo Laboratory (Guenthner et al. 2013). FosTRAP mice were obtained from a colony created by the Jackson Laboratory (JAX Mice & Services, Bar Harbor, ME). The Jackson Laboratory mated homozygous Ai14 females (JAX Mice & Services, Stock No. 007914) with heterozygous Fos^{CreER} males (JAX Mice & Services, Stock No. 021882). FosTRAP mice are the offspring that are heterozygous for both the *R26-Ai14* gene and the *Fos-CreER* gene. The Ai14 mice have a *tdTomato* gene linked to the Cytomegalovirus early enhancer/chicken beta actin (CAG) promoter that is floxed with a loxP-STOP-loxP cassette. Heterozygous Fos^{CreER} mice have a $CreER^{T2}$ gene knocked into one of the Fos promoters. FosTRAP utilizes tamoxifen-dependent recombinase, $CreER^{T2}$, expressed in an activity-dependent manner through the Fos promoter that recombines with 4-hydroxytamoxifen (4-OHT, Sigma-Aldrich Corp., St. Louis, MO, Cat. No. H6278) to unlock a STOP-floxed *tdTomato* gene. The *tdTomato* gene that was unlocked by activity during the metabolically active 4-OHT time window (~6 h) will then continually express to label active neurons even after c-Fos expression starts fading (2 h) (Gao and Ji 2009; Guenthner et al. 2013; Hunt et al. 1987). Activity by other neurons outside of this time window will not express tdTomato because there is no 4-OHT to recombine with subsequent activity-related $CreER^{T2}$ expression to unlock their *tdTomato* gene. This allows genetic access of neural activation during desired time frames that can then be compared with c-Fos expressed during a later event. It must be noted that a new version of the FosTRAP mouse, named TRAP2, has since been developed after our experiments were completed (JAX Mice & Services, Stock No. 030323) (DeNardo et al. 2019). All procedures were performed according to institutional and governmental regulations and in accordance with the guidelines delineated by the University of California, Los Angeles, Chancellor's Animal Research Committee, concerning the ethical use of animals. A total of 47 adult (6–12 mo old) FosTRAP mice were used for all experiments described in this study.

Experimental design. The first experiment optimized the injection timing of 4-OHT that best captured neural activation from 30 min (20.0 cm/s) of stepping on a treadmill. Adult FosTRAP mice were divided among different injection time points relative to the beginning of stepping: 4 h before stepping (−4 h, $n = 1$), 2 h before stepping (−2 h, $n = 2$), 1 h before stepping (−1 h, $n = 2$), immediately before stepping (0 h, $n = 6$), immediately after the completion of stepping (+0.5 h, $n = 7$), and 1 h after the completion of stepping (+1.5 h, $n = 3$). There was also a group of FosTRAP that received a sham intraperitoneal injection (vehicle w/o 4-OHT, $n = 2$). All groups received 4-OHT intraperitoneal injections at a dosage of 75 mg/kg. The 4-OHT solution was made by dissolving 4-OHT in 100% ethanol, suspended in castor oil, stored in −20°C, and then thawed and mixed with injectable saline for experimental use (Chevalier et al. 2014). All mice were acclimated to stepping on a treadmill for 30 min on five different occasions before stepping and receiving a 4-OHT injection. After stepping for 30 min on a treadmill (two 15-min sessions with a 5-min break in between sessions), the mice were returned to their cages. FosTRAP mice remained in their cages for 14 days to allow for tdTomato production and subsequent diffusion. After 14 days, mice stepped for another 30 min on a treadmill under the same conditions as before. Note that no tdTomato will capture the activity due to the second bout of stepping because there is no 4-OHT injection for this event. One hour after the completion of stepping, mice were transcardially perfused with 4% paraformaldehyde (PFA, Sigma-Aldrich, Cat. No. 158127) in phosphate buffer. Mice that could not complete stepping at 20 cm/s for the 30-min period were omitted from the analysis.

The second experiment optimized the dosage of 4-OHT that best captured neural activation from 30 min of stepping (20.0 cm/s) on a treadmill. Adult FosTRAP mice were divided among different injection dosages: 0 mg/kg (sham, $n = 2$), 25 mg/kg ($n = 1$), 50 mg/kg ($n = 2$), and 75 mg/kg ($n = 3$). The dosage was capped at 75 mg/kg because of a previous finding in which 100 mg/kg was lethal (Guenthner et al. 2013). All animals received their 4-OHT injection immediately after stepping, the optimal injection time found in the previous experiment. Mice stepped on the treadmill for 30 min, under the same conditions as

the previous experiment, and were put back in their cages for 14 days. After 14 days, mice stepped on a treadmill for 30 min and were transcardially perfused with 4% PFA 1 h after the completion of stepping.

The third experiment compared and contrasted c-Fos and tdTomato activation for repeated bouts of stepping (20 cm/s) and for stepping versus resting. The stepping condition was the same as described for the previous experiments. The resting condition was captured after 8:30 AM when the mice were asleep. For resting tdTomato, mice were injected with 4-OHT at 8:30 AM and their activity was monitored every 10 min for 7 h to make sure they were not particularly active. Mice that were overly active during this 7-h period were discarded from this group. For resting c-Fos, mice were euthanized 1 h after a 2-h period of rest was observed in the morning. At *day 0*, the animal performed either stepping or resting for *task 1* and then received a 4-OHT injection (75 mg/kg) upon completion (Fig. 1). After 14 days, the mice performed stepping or resting for *task 2* and then were transcardially perfused with 4% PFA 1 h after completion of *task 2*. Before *task 1*, all animals were acclimated to the treadmill as in previous experiments. Neural activation due to *task 1* is labeled with tdTomato, and neural activation due to *task 2* is labeled with c-Fos. The three experimental groups can be seen in Fig. 3. The first group compares tdTomato and c-Fos activation due to stepping for 30 min on a treadmill (St vs. St, $n = 8$). The second group compares resting (R, marked with tdTomato) and stepping (St, marked with c-Fos) and is denoted as R versus St ($n = 4$). The third group compares stepping (St, marked with tdTomato) and resting (R, marked with c-Fos) and is denoted as St versus R ($n = 4$).

Tissue preparation. After perfusion with 4% PFA, the spinal cords were dissected and postfixed overnight in 4% PFA at 4°C. Spinal cords were then put in 30% sucrose for 5 days at 4°C and divided into a segment spanning the L1–L6 spinal levels, which was then frozen with Neg 50 (Thermo Scientific, Hudson, NH). These blocks were then stored in −80°C until they were ready to be cut into 30-μm sections with a cryostat. Tissue sections were stored in 96-well plates with 1× phosphate-buffered saline (PBS) and 0.02% sodium azide at 4°C.

Immunohistochemistry. Sections from spinal level, L4, were examined for this study. L4 sections were identified based upon the morphology of the gray and white matter using an atlas (Watson et al. 2009). Twelve to 15 sections, sampled at every fourth section, underwent immunohistochemical analysis. The sections sampled spanned rostral, middle, and caudal sections of L4. Goat anti-

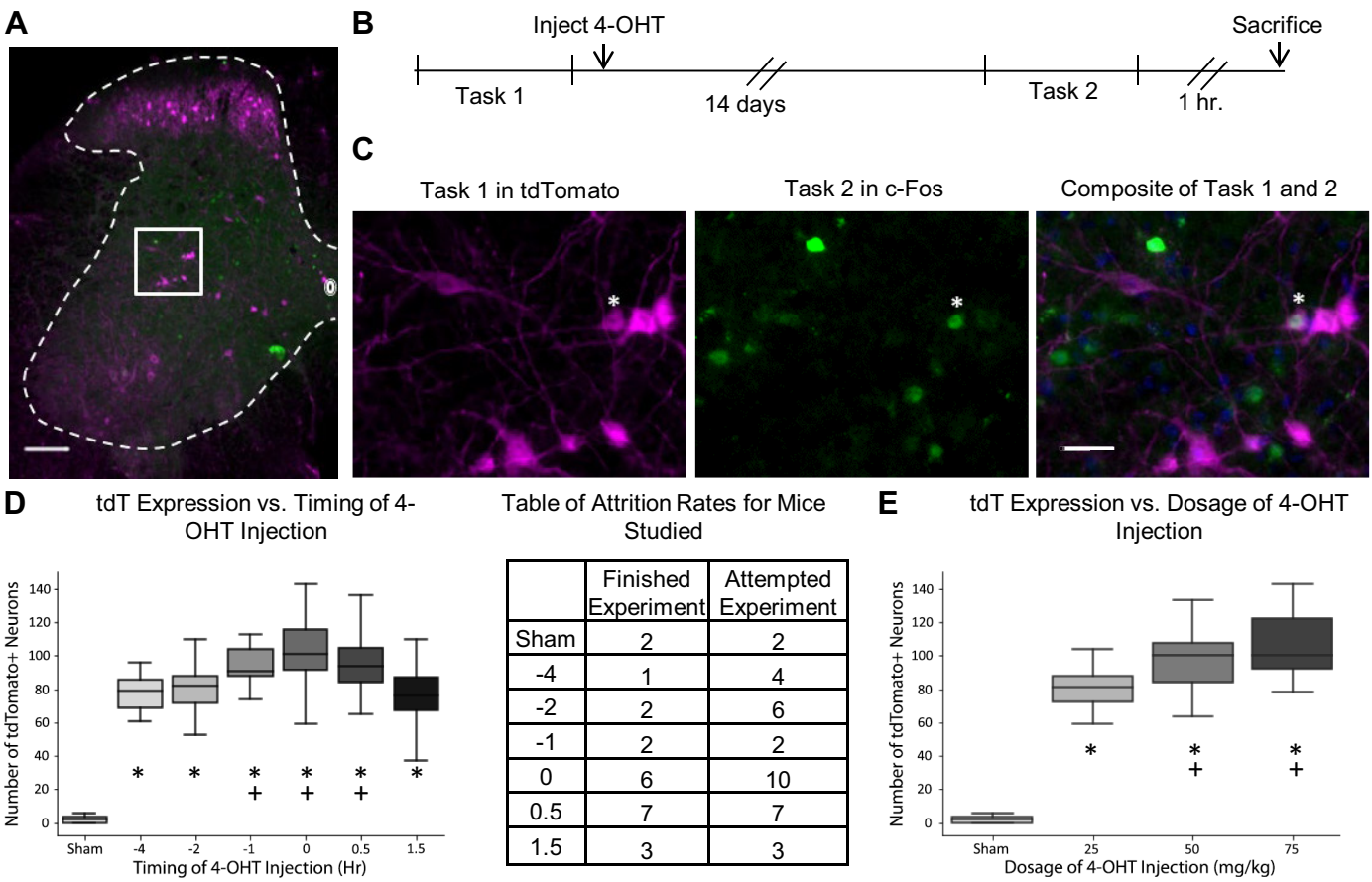

	Finished Experiment	Attempted Experiment
Sham	2	2
-4	1	4
-2	2	6
-1	2	2
0	6	10
0.5	7	7
1.5	3	3

Fig. 1. Experimental design, visualization, and optimization. *A*: composite image of TRAP mouse L4 section after completing *task 1* and *task 2*. Tasks are either stepping for 30 min on a treadmill or resting cage activity. In this figure, *tasks 1* and *2* are both stepping. *B*: experimental timeline. *C*: visualization of boxed area in *A* decomposed into separate channels and locomotor tasks. Asterisk denotes a colabeled neuron (c-Fos+ and tdTomato+) that has been active during *task 1* and *task 2*. Scale bars in *A* and *C* are 100 μm and 25 μm, respectively. *D*: number of neurons labeled with tdTomato (tdT) with the timing of 4-OHT injection. The *x*-axis shows the time of 4-OHT injection in hours relative to the beginning of stepping, marked at 0. The table shows the number of mice that completed the task for 30 min and the number of mice attempted. Asterisks denote groups that are significantly different from the sham group (Tukey's $P = 0.001$ for all groups; Tukey's $q = 14.57$, 16.89, 19.59, 25.98, 25.51, and 18.24, respectively, for −4-, −2-, −1-, 0-, 0.5-, and 1.5-h groups). Plus signs denote groups significantly different from the 1.5-h group (Tukey's $P = 0.01$, 0.001, and 0.001; Tukey's $q = 4.92$, 8.54, and 7.56, respectively, for the −1-, 0-, and 0.5-h groups). *E*: comparing the number of tdTomato+ neurons with the dosage of 4-OHT (mg/kg). Asterisks denote groups that are significantly different from the sham group (Tukey's $P = 0.001$ for all groups; Tukey's $q = 19.82$, 26.64, and 29.21, respectively, for the 25, 50, and 75 mg/kg groups). Plus signs denote groups that are significantly different from the 25 mg/kg group (Tukey's $P = 0.021$ and 0.001; Tukey's $q = 4.18$ and 6.24, respectively, for 50 and 75 mg/kg groups). 4-OHT, 4-hydroxytamoxifen; TRAP, targeted recombination in active populations.

tdTomato antibody (1:4,000, LS Bio, Seattle, WA; Cat. No. LS-C340696) amplified tdTomato produced during *task 1*, and rabbit anti-c-Fos (1:2,000, EMD Millipore, Burlington, MA; Cat. No. ABE457) identified active neurons during *task 2*. Neurons double-labeled with both tdTomato and c-Fos indicated neurons activated by both *task 1* and *task 2* and were called colabels. The chosen sections underwent immunohistochemistry as free-floating sections, similar to previous studies (Ahn et al. 2006; Tillakaratne et al. 2014). Briefly, sections were transferred into Costar netwells (15-mm membrane diameter and 74-μm mesh), rinsed for 30 min in 1× PBS, transferred to 96-well plates containing 180 μL/well of a mixture of c-Fos and tdTomato antibodies in 1× PBS containing 0.3% Triton X-100 and 5% normal donkey serum (NDS), and incubated for 3 days at 4°C on an orbital shaker. Afterward, sections were washed in 1× PBS as follows: two quick rinses, two 5-min rinses, and two 10-min rinses. Sections were incubated in a mixture (180 μL/well, 96-well plate) of secondary antibodies (donkey anti-rabbit 488 at 1:500 and donkey anti-goat 594 at 1:500 from Jackson ImmunoResearch, West Grove, PA, Code: 711–545–152 and 705–585–147, respectively) in 0.3% Triton X-100 and 5% NDS for 1 h at room temperature on an orbital shaker. After secondary antibody incubation, sections were washed in 1× PBS as described earlier after primary antibody incubation, mounted on Fisher Superfrost slides (Fisher Scientific, Pittsburgh, PA), and coverslipped with VECTASHIELD mounting media containing DAPI (4′,6-diamidino-2-phenylindole) (Vector, Burlingame, CA).

Quantification and data analyses. Spinal cord sections processed for fluorescent immunohistochemistry were examined under a Zeiss Axiophot microscope with appropriate fluorescent filter sets. Digital images of neurons labeled with c-Fos, DAPI, and tdTomato were acquired with a Spot RT CCD Slider color camera (Diagnostics Instruments, Sterling Heights, MI) and using extended field of depth imaging in Image Pro Plus 7 (Media Cybernetics, Rockville, MD). Composite images of c-Fos, DAPI, and tdTomato were created with the color composite feature of Image Pro Plus 7. Neurons that expressed c-fos, tdTomato, or both were tagged using the manual tag analytical feature of Image Pro Plus 7. The manual tags were then exported to Microsoft Excel as *x, y* coordinates. Sections from the same animal had their points shifted and aligned with the central canal as a fiducial structure. These points were then uploaded using the Tableau Software (Tableau Software, Seattle, WA), and the laminae borders (Watson et al. 2009) were overlaid onto the manual tag points. Tableau was then able to count the number of c-Fos, tdTomato, or colabeled neurons in each lamina. Total c-Fos activation was the sum of the number of c-Fos positive neurons and the number of colabeled neurons per section. Similarly, total tdTomato activation was the sum of the number of tdTomato positive neurons and the number of colabeled neurons. Colabeling percentage was calculated by dividing the number of colabels by the total tdTomato activation and multiplying by 100. To visualize the spatial distribution of c-Fos and tdTomato, a heat map over the *x* and *y* coordinates of the section was generated using a kernel density estimate (KDE), which was done using the R software package (R Foundation for Statistical Computing, Vienna, Austria, http://www.R-project.org). All quantification was performed blindly by assigning a code letter to each animal and deciphering this code only after all data analyses were complete. The data were derived and reported from 16 mice with 12–15 tissue sections taken from each mouse. A total of 17,008 tdTomato+ and 18,702 c-Fos+ neurons were identified with respect to their *x-y* position in the spinal gray matter.

Statistical analyses. Mean comparisons of the groups in *experiments 1, 2*, and *3* were carried out using a factorial one-way analysis of variance (ANOVA) model with a Tukey honestly significant difference (HSD) post hoc analysis (Figs. 1 and 3). The statistical analysis on the distribution of c-Fos, tdTomato, and colabels from the third experiment used resampling techniques (Miller et al. 2010). Also, *x, y* coordinates, for a particular activity marker (c-Fos or tdTomato) activated by a certain locomotor condition (resting and stepping) from all sections and animals, were registered and aligned to the central canal and compiled into a single list. This list was then resampled (with replacement) 1,000 times to create a heat map with a 95% confidence interval at each location. The confidence interval would be compared with another group's (activity marker + locomotor condition) heat map. Spatial locations of the compared group's heat map that were outside this confidence interval were considered significantly different. For this study, two different comparisons were made: spatial distribution and spatial counts. Spatial distribution tested the question whether two conditions (e.g., stepping c-Fos vs. stepping tdTomato, stepping c-Fos vs. resting c-Fos) came from the same underlying spatial distribution. In this analysis, resampling was done so that the number of *x, y* coordinates in the compared groups was the same. For example, there were more c-Fos+ neurons than tdTomato+ neurons for stepping. The *x, y* coordinate list for tdTomato was up-sampled with replacement to match the number of *x, y* coordinates for c-Fos, and this was done 1,000 times to create the confidence interval. As the numbers of coordinates in the compared groups were the same, this analysis revealed proportionality differences between the two groups. In contrast, spatial count analysis determined whether the absolute counts of neurons at a particular location were the same for the compared groups. In this case, the number of *x, y* coordinates in the resampled list matched that of the original list. Using the same example as earlier, the tdTomato coordinate list was not up-sampled with replacement to match the length of the c-Fos coordinate list but resampled to the same length of the original tdTomato list, and this was done 1,000 times to create the confidence interval. Resampling was carried out using the R programming language.

RESULTS

4-OHT injection (75 mg/kg) of FosTRAP mice immediately after the end of locomotor activity produced robust tdTomato labeling of active neurons. For the dosage optimization experiment, all dosages of 4-hydroxytamoxifen (4-OHT) resulted in significantly higher tdTomato expression than the sham injection, with 75 mg/kg having the highest amount of tdTomato expression (Fig. 1*E*). Higher dosages (100 mg/kg) were not used because of the lethality of 4-OHT on mice as previously studied (Guenthner et al. 2013). The sham group expressed very little and sparse tdTomato, thus showing that the FosTRAP model is tightly modulated with 4-OHT and shows little expression because of events outside an intended time window. For the timing optimization experiment, all injection time points (excluding the 1.5-h group) resulted in similar amounts of tdTomato expression, suggesting that the exact timing of 4-OHT did not matter as long as it occurred before the end of stepping (Fig. 1*D*). However, the 4-OHT injection noticeably hindered the animals' ability to complete locomotor tasks, resulting in high attrition rates when injected before the onset of locomotion. These animals displayed characteristics like sluggishness and social isolation in the time leading up to the experiment and often would completely stop stepping on the treadmill. These abnormalities subsided once the 4-OHT had cleared their systems. For subsequent experiments, we injected 4-OHT at 75 mg/kg immediately after the end of the locomotor task. These parameters showed robust tdTomato labeling while also minimizing attrition rate.

"TRAPed" neurons expressed tdTomato that labeled the soma and processes. "TRAPed" neurons first express tdTomato in the nucleus, and if given enough time, it can accumulate and spread to the soma and processes. This was especially noticeable after amplifying tdTomato with immunostaining (Fig. 1, Supplemental Videos S1 and S2; all Supplemental material is available at

https://doi.org/10.6084/m9.figshare.12448616). TRAP appeared to label glia in the spinal cord white matter with the morphology correlating to either oligodendrocytes or astrocytes, both of which have been shown to produce c-Fos (Groves et al. 2018; Muir and Compston 1996). However, confirmation with oligodendrocyte or astrocyte biomarkers was not done. Tissue-clearing techniques, like clear lipid-exchanged acrylamide-hybridized rigid imaging/immunostaining/in situ hybridization-compatible tissue hydrogel (CLARITY), further enhance FosTRAP's (Supplemental Videos S1 and S2) ability to reveal processes of activated neurons and have the potential to reveal some degree of anatomical proximity of activated spinal networks that a nuclear c-Fos (Supplemental Videos S3 and S4) stain cannot show. Furthermore, this can be combined with biomarkers for genetic lineages like Chx10 (Supplemental Videos S5 and S6) to uncover system-wide activation and connectivity of genetically distinct interneurons, potentially revealing their multifunctional nature in executing different motor tasks.

TdTomato captured spatial differences between stepping and resting similar to c-Fos. The differences in spatial activation patterns for stepping versus resting were consistent for c-Fos and tdTomato. Two-dimensional kernel density estimates (KDEs) were used to visualize the distribution and counts of activated neurons and give the probability of finding c-Fos or tdTomato at each spatial location. Each KDE was normalized with respect to itself (i.e., the probabilities were with respect to sections found in that particular animal), and thus, each KDE showed proportionate spatial activation patterns for that animal. Resting showed higher proportionate activation around the central canal and medial laminae V-VII, whereas stepping showed higher proportionate activation in the lateral dorsal horn and lateral intermediate laminae (Fig. 2*A2*). However, stepping showed higher spatial counts throughout all the gray matter, with the greatest difference found in the medial dorsal horn and laminae IV, V, and VII (Fig. 2*B2*, Supplemental Fig. S1). TdTomato showed similar differences between resting and stepping as c-fos (Fig. 2, *A2* and *A3*).

Expression levels of tdTomato and c-Fos differed when both were activated by the same locomotor task. TdTomato and c-fos counts significantly differed when both capture the same activity (e.g., tdTomato stepping vs. c-Fos stepping). c-Fos showed more activation in response to stepping than tdTomato, and the opposite was true for the resting condition (Fig. 3). c-Fos shows a greater numerical difference in expression between the resting and stepping conditions than does tdTomato. These results could arise because of the differences in how c-Fos and tdTomato are expressed (see DISCUSSION).

Despite the *Fos-Cre* link, tdTomato had different spatial distributions and counts than c-Fos when activated by stepping. c-Fos shows increased activation in the medial dorsal horn and in the intermediate laminae, whereas tdTomato shows increased activation throughout the dorsal horn with the intermediate laminae showing less activation (Fig. 2*A1*). For stepping, tdTomato activation showed proportionately higher activation than c-Fos in the dorsal and ventral horns, and c-Fos showed proportionately higher activation around the central canal and intermediate layers (*right*, Fig. 4*A*). c-Fos and tdTomato also had different spatial counts. TdTomato showed fewer neurons activated when going from dorsal to ventral horn, whereas c-Fos shows peak activation in the medial dorsal horn and medial intermediate laminae (Fig. 2*B1*, Supplemental Fig. S1). Overall, c-Fos outnumbers tdTomato in almost all layers of the spinal cord except for small areas in the ventral horn and lateral dorsal horn (*right*, Fig. 4*B*). For resting, c-Fos showed a higher proportional activation around the central canal and medial intermediate layers, and tdTomato shows a higher proportional activation in the dorsal and ventral horn (*left*, Fig. 4*A*). TdTomato shows higher spatial counts at rest than c-Fos in all laminae except V and VI with the greatest discrepancy found in the dorsal horn (*left*, Fig. 4*B*, Supplemental Fig. S1).

FosTRAP mice showed more colabeling (positive for tdTomato and c-Fos) when repeating the same stepping task than when comparing stepping and resting. Neurons colabeled with c-Fos and tdTomato revealed unique perspectives in how neural networks execute repeated versus different tasks. The experimental design for this analysis is shown in Fig. 1. Repeating the same task (St vs. St) had a higher number of colabels compared with performing two different tasks (R vs. St) (Fig. 5). The St versus St and R versus St groups also have different spatial distributions of colabeling. The R versus St group had most of its colabeling in the dorsal half of the spinal cord, whereas the colabeling in the St versus St group can be seen throughout the gray matter. Most notably, the St versus St group showed colabeling in the ventral horn, whereas the R versus St group did not.

The use of FosTRAP suggests redundancy among spinal networks when repeating two 30-min bouts of treadmill stepping. The FosTRAP model suggests an interesting property of spinal networks when repeating the execution of a similar task. On average, ~20% of the neurons that expressed tdTomato during the first bout of stepping were also positive for c-Fos after the second bout of stepping (thick trace in Fig. 6, *A* and *C*). Individual one-dimensional (1-D) kernel density estimates (KDEs) (thin traces in Fig. 6) were created from sections in the L4 spinal segment collected from each animal. These individual KDEs showed a range of colabeling (tdTomato+ and c-Fos+) rates even within the same spinal segment. The peaks of the individual KDEs ranged from ~10% to 25%. This level of colabeling with repeated bouts of stepping becomes even more surprising, considering that each 30-min stepping period at 20.0 cm/s consisted of ~7,000 step cycles performed. The phenomenon of neural variability of repeated tasks in the spinal cord has implications for how we view the sensory-motor interactions of spinal networks in vivo.

DISCUSSION

The activation patterns of spinal neurons during locomotion have been studied using c-Fos labeling in rats, mice, and cats (Ahn et al. 2006; Barajon et al. 1992; Courtine et al. 2008; Dai et al. 2005; Dale et al. 2014; De Leon et al. 1998; 1999; Huang et al. 2000; Ichiyama et al. 2008; Kim et al. 2013). The targeted recombination in active populations (TRAP) mouse model provides a tool to compare neuronal network activation during two instances of movement in the same animal. Thus far, FosTRAP has been used to probe network activity from somatosensory and visual stimuli in the brain along with fear-conditioning paradigms (Allen et al. 2017; Cazzulino et al. 2016; Chatzi et al. 2019; DeNardo et al. 2019; Girasole et al. 2018; Guenthner et al. 2013; Joshi and Panicker 2018; Tasaka et al. 2018; Ye et al. 2016). In this study, TRAP mice were used to compare populations of active neurons in the spinal cord when repeating the

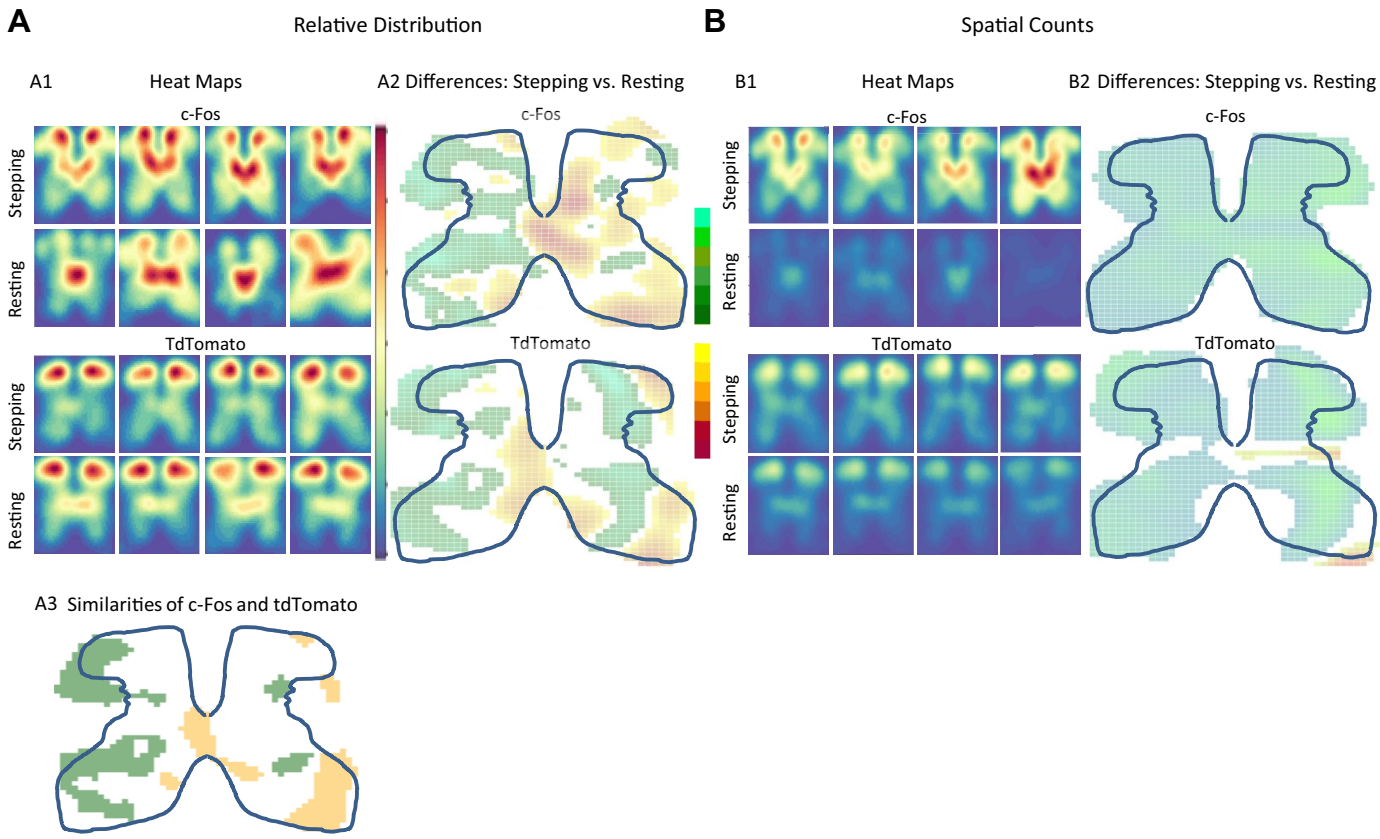

Fig. 2. Relative spatial distribution and counts based on tdTomato and c-Fos. *A1*: relative spatial distribution heat maps for c-Fos stepping and resting (*top* half) and for tdTomato (*bottom* half) from four representative animals. Red areas represent higher probability. Each panel is a heat map generated from all tissue sections for each mouse. The heat maps generated from all animals tested can be found in Supplemental Fig S2. *A2*: the relative distribution differences between stepping and resting as captured by either c-Fos (*top*) or tdTomato (*bottom*). Red areas represent where resting has significantly higher probability than stepping, and green areas represent where stepping has significantly higher probability than resting. *A3*: similarities of c-Fos and tdTomato when comparing stepping versus resting. This panel is derived from *A2*. Yellow denotes areas where c-Fos and tdTomato both detect greater activation from resting compared with stepping, and green denotes areas where c-Fos and tdTomato both detect greater activation from stepping compared with resting. *B*: heat maps and differences based on spatial counts of neurons after stepping and resting as captured by either c-Fos or tdTomato. Otherwise, all descriptions noted for *A* apply to *B*, except that the spatial count heat maps from all mice tested can be found in Supplemental Fig. S3. Statistical significance was determined through resampling techniques in which a 95% confidence interval was created (see METHODS).

same stepping task, as well as comparing the population of active neurons during stepping and resting.

The present results show that FosTRAP can capture activation differences between two different events in the spinal cord, analyze the activation patterns of TRAP and c-Fos, and suggest a system-wide level of probabilistic activation of spinal networks performing the same motor task. The observation that only 20% of the active neurons were colabeled when performing ~7,000 steps on a treadmill on two separate occasions leaves open the possibility that a vast range of different combinations of neurons can generate thousands of steps with each one being biomechanically similar, but substantially different neurally (Musienko et al. 2012). This result contrasts with a previous finding using FosTRAP to study a sensory system in which a 70% colabeling rate was found in neurons activated by identical pure tone stimuli in the cochlear nuclei (Guenthner et al. 2013). Our result is consistent with previous findings of multiple combinations of neural networks that can perform the same motor action such as stepping (Latash and Zatsiorsky 2016). The key question is just how many combinations are available to perform the thousands of steps. This level of variability in the motor system could have several physiological advantages. The FosTRAP model provides a tool that can be used in the future experiments to study many different aspects of spinal physiology.

TdTomato captures spatial differences between stepping and resting. TdTomato can capture activity patterns that are unique to different locomotor events in the spinal cord. At first glance, the spatial distributions of tdTomato stepping and resting qualitatively look similar. However, quantitatively, the spatial patterns differed significantly between stepping and resting. In addition, c-Fos shows similar quantitative differences between stepping and resting (Fig. 2, *A3* and *B2*). This indicates that both c-Fos and tdTomato captured relatively similar spatial encoding differences between stepping and resting. This result shows that FosTRAP can capture complex experiences, like stepping, in the spinal cord as well as complex experiences, like fear-conditioning and maternal auditory processing, in the brain (Allen et al. 2017; Cazzulino et al. 2016; DeNardo et al. 2019; Tasaka et al. 2018; Ye et al. 2016). However, there are some differing features between tdTomato and c-Fos activation.

Differences in tdTomato and c-Fos activation patterns when capturing the same task. Despite tdTomato and c-Fos being activated by the Fos promoter, tdTomato and c-Fos differ in

A Cell counts of Groups Comparing Motor Tasks

Group	Task 1 (tdT)	Task 2 (c-Fos)	tdT	c-Fos	colabel
St vs. St (n = 8)	Stepping	Stepping	98.2 SD 10.2	149.6 SD 44.9	19.9 SD 4.2
St. vs. R (n=4)	Stepping	Resting	84.5 SD 8.7	38.1 SD 8.1	3.6 SD 1.0
R vs. St (n=4)	Resting	Stepping	68.9 SD 2.9	157.9 SD 14.1	11.6 SD 2.9

B c-Fos and tdTomato Counts of Resting or Stepping

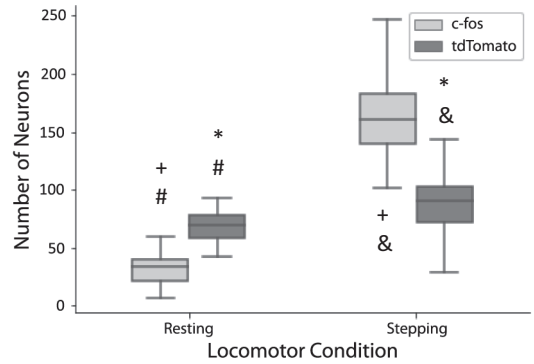

Fig. 3. *A*: table showing the mean and standard deviations of c-Fos, tdTomato (tdT), and colabeling counts per spinal section from each experimental group. *B*: box plot of c-Fos and tdTomato expressed per spinal section during either resting or 30 min of stepping. Values were calculated from experimental groups in *A* (e.g., tdTomato stepping calculated from groups St vs. St and St vs. R). Box plots marked with * (Tukey's $P = 0.001$, Tukey's q = 6.94), # (Tukey's $P = 0.001$, Tukey's q = 9.66), & (Tukey's $P = 0.001$, Tukey's q = 30.38), and + (Tukey's $P = 0.001$, Tukey's q = 40.68) are significantly different from each other using Tukey's HSD post hoc analysis after a one-way ANOVA for all sections from all animals under the resting or stepping condition.

number and distribution while capturing the same condition (Figs. 3 and 4). Particularly, tdTomato captures fewer active neurons in the medial intermediate laminae compared with c-Fos (Fig. 4*A*). The number of tdTomato+ and c-Fos+ neurons could differ because of *1*) the length of time that 4-OHT stays in the system and *2*) its longer pathway to expression than c-Fos. TdTomato captures network activity on a longer timescale than c-Fos (6 h vs. ~1.5 h) resulting from the length of time 4-OHT stays in the system. The longer time window of 4-OHT manifests itself in the timing optimization experiments where stepping tdTomato expression does not differ with time (Fig. 1*D*) and can also be seen in the higher tdTomato counts than c-Fos during resting where tdTomato records 6 h of "resting" (Figs. 2*B1* and 3, Supplemental Fig. S1). In this study, tdTomato only captures treadmill stepping for 30 min out of a ~6-h recording window, in which the other ~5.5 h recorded within this window was considered "resting" (compared with ~6 h of rest for the resting condition). This similarity between the resting and stepping conditions could lead to the muted difference in the total number of tdTomato+ neurons between these two conditions as compared with c-Fos (Fig. 3*B*). To make up for tdTomato capturing less active neurons than c-Fos, the original FosTRAP experiments provided a longer stimulus for the "TRAPed" condition to record (4-h stimulus) compared with the

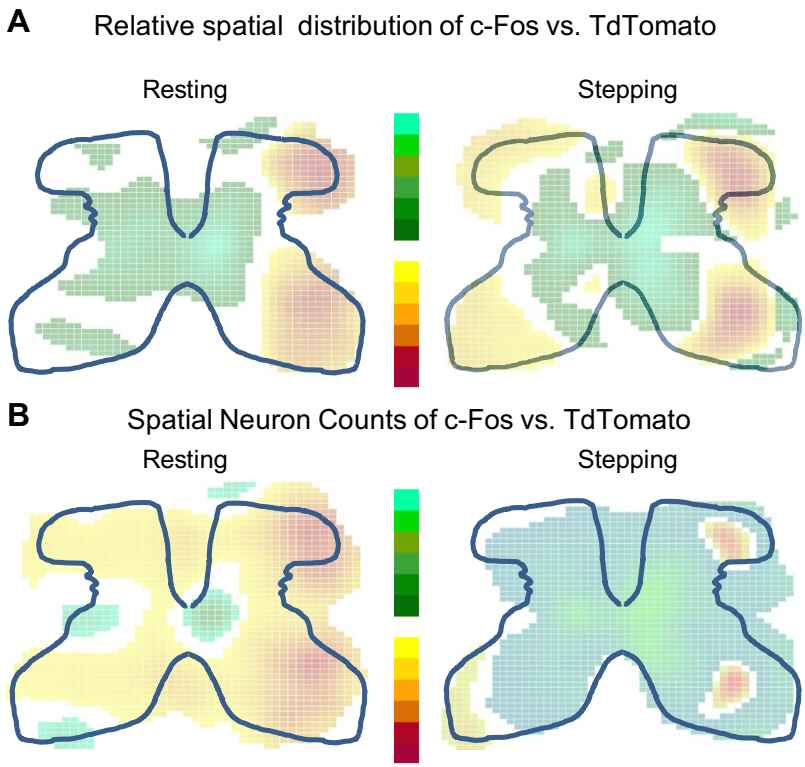

Fig. 4. Differences in spatial distribution and counts of c-Fos and tdTomato when activated by resting or stepping. *A*: map of the differences in spatial distribution between c-Fos and tdTomato during resting or stepping calculated from KDEs shown in Fig. 2 and Supplemental Fig. S2. *B*: map of the differences in spatial counts between c-Fos and tdTomato during resting or stepping calculated from KDEs shown in Fig. 2 and Supplemental Fig. S3. For both *A* and *B*, green represents areas where c-Fos is significantly higher and red represents areas where tdTomato is significantly higher. White represents areas of no significant differences. Statistical significance was determined through resampling techniques in which a 95% confidence interval was created (see METHODS). KDE, kernel density estimate.

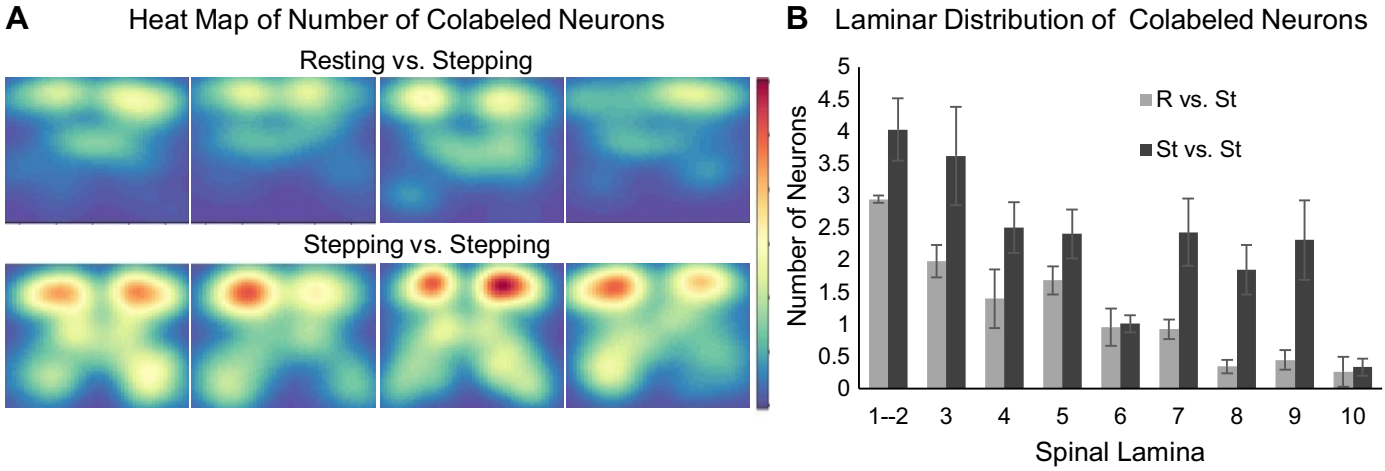

Fig. 5. Distribution and counts of colabeling. *A*: spatial count heat maps of colabeled neurons in the resting versus stepping (R vs. St) and stepping versus stepping (St vs. St) experimental groups. Red labels areas with higher neuronal counts, and blue labels areas with lower neuronal counts. *B*: histogram of colabeling number of neurons by spinal laminae.

condition captured by c-Fos (1-h stimulus) (Guenthner et al. 2013). Moreover, tdTomato's longer reaction pathway could result in it having a different activity threshold. The expression of tdTomato requires extra steps compared with that of c-Fos, including recombination of *Fos*-linked CreER with 4-OHT and then subsequent targeting of a floxed *tdTomato* gene by the recombined product. Because of the probabilistic nature of biochemical reactions, to form more product (tdTomato), a higher concentration of reactants (i.e., CreER) is needed, which requires an elevated activity-dependent production of CreER. These factors could lead to tdTomato having a different activity threshold compared with that of c-Fos.

Colabeling in FosTRAP mice implies redundancy and multifunctionality in spinal networks. The methodology here provides a way to explore redundancy and interneuronal multifunctionality at a system-wide level in unconstrained in vivo locomotor behavior. The presence of colabeling in the performance of two different tasks, especially ones as different as resting and stepping, is consistent with previous studies demonstrating the multifunctional nature of spinal interneurons (Berkowitz 2010; Berkowitz et al. 2010; Briggman and Kristan 2008; Esposito et al. 2014; Hao and Berkowitz 2017; Jankowska 2001; Levine et al. 2014). This multifunctionality would be expected to facilitate the spinal cord's ability to easily learn and remember a wide range of movement patterns such as cycling, swimming, and stepping. Recordings of single cells being activated during different types of motor activity (Berkowitz 2010; Berkowitz et al. 2010; Hao and Berkowitz 2017; Jankowska 2001) or single-cell stimulation eliciting activation of multiple muscles (Levine et al. 2014) from previous studies are consistent with the present observation of multifunctionality from the colabeling results. However, they do not address the question of how often the same combination of neurons is activated in a repetitive task requiring thousands of cycles on two occasions.

Previous studies have used single-unit electrophysiological recordings to investigate the execution of similar motor tasks elicited by different stimulation techniques (Musienko et al. 2020) or under different postural conditions (Deliagina et al. 2012; Zelenin et al. 2015, 2016). For example, Musienko et al. (2020) reported that 50% of the recorded spinal neurons showed similar and stable modulation when stepping was elicited by epidural or mesencephalic locomotor region (MLR) stimulation.

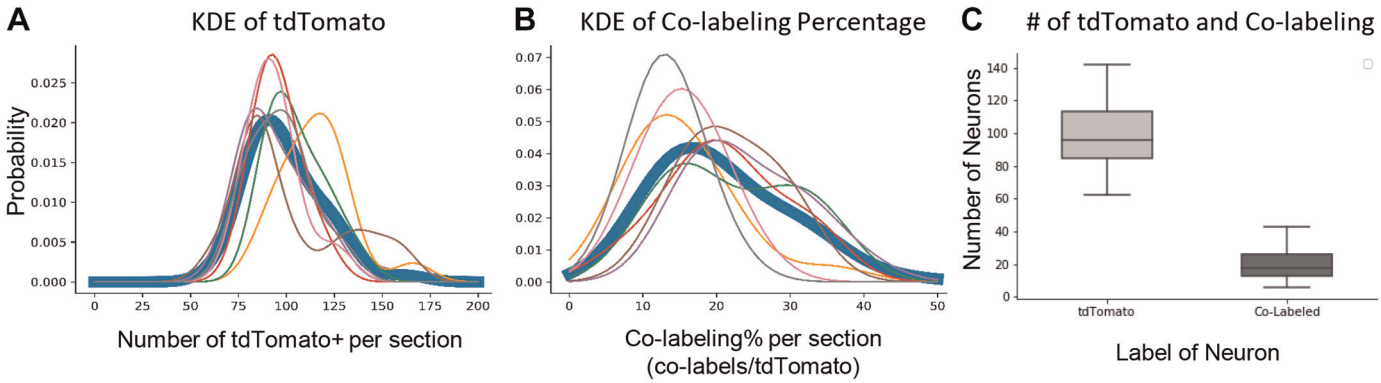

Fig. 6. Rate of colabeling in the tdTomato+ population because of repeated bouts of stepping. *A*: kernel density estimates (KDEs) showing the distribution of tdTomato+ counts per section for all sections gathered from a single animal (thin trace) or all sections gathered from all animals (thick trace). *B*: KDEs for the percentage of tdTomato+ neurons that are colabeled per section. Thin and thick traces hold the same convention as in *A*. *C*: box plot of the tdTomato+ counts per section and the number of colabels per section across all sections from all animals.

These methodologies were performed in surgically reduced (decerebrated) animals that were stabilized in a fixed-body constraint. Also, electrophysiological approaches limit the number of neurons that can be observed because of volumetric constraints. But even given the disparity between the present experimental strategies and that of Musienko et al., both studies are consistent with the interpretation that the same set of neurons could be rarely repeated in stepping (even at the same speed). Our estimation of 20%, however, may be biased toward a lower level of colabeling than the true percentage because of tdTomato undersampling neural activity during stepping compared with c-Fos.

Factors like the two running tasks tested not being completely "identical" and that some spontaneous neural plasticity could have occurred between the times that each animal was tested could have contributed to the level of colabeling observed. Even though two bouts of stepping at a fixed speed were performed, these bouts are not neurally, kinematically, or kinetically "identical" (Bernshteĭn 1967). Not having the body fixed (Musienko et al. 2020) reflects a more real-life scenario but will cause postural and strategic variation (Bellardita and Kiehn 2015; McLean et al. 2008), which can lead to a different sensory processing and thus different kinematics (Deliagina et al. 2012; Gerasimenko et al. 2017; Lavrov et al. 2008; Zelenin et al. 2015, 2016). The half-life of synaptic proteins can be on the order of hours to weeks, and this turnaround results in homeostatic reweighting of the network (Marder and Goaillard 2006). However, to maintain the network's intended function, the homeostatic upkeep of the synapses would not be expected to completely explain the colabeling rate found in our study.

Though neural variability inevitably leads to variations in the kinetics and kinematics of a step, this feature could theoretically be advantageous in providing an *1*) adaptive mechanism to perturbations through movements with differing kinetics and kinematics that can perform the same task, *2*) a design that would minimize synaptic fatigue, and *3*) a physiological and anatomical platform that provides mechanisms for reorganization of networks when there is a neuromuscular injury. From this perspective, epidural and transcutaneous stimulation experiments combined with physical rehabilitation may be able to facilitate and engage many options in reorganizing spinal networks (Ichiyama et al. 2008; Lavrov et al. 2008). Providing some limited level of variability in step training compared with a fixed trajectory results in more robust recovery after spinal cord injury (Shah et al. 2012; Ziegler et al. 2010). The variable recruitment of different spinal neural networks suggested in this study is consistent with the observations of Cai et al. (2006) and Ziegler et al. (2010) that using an "assist as needed" robotic training method to facilitate repetitive step cycles is more effective in improving unaided stepping than imposing the same trajectory for every step. The improved outcomes could stem from engaging a wider range of redundant spinal networks that can execute stepping. The results, however, are not definitive, and thus, further studies are needed to clarify the limitations of the FosTRAP model to draw stronger conclusions about the level of redundancy among spinal networks.

Limitations. Guenthner et al. (2013) have outlined some of the limitations of FosTRAP, which derive from using c-Fos as an activity marker, where it has been found to be underrepresented in certain areas and neuronal phenotypes. Further clarification experiments on tdTomato's under-sampling can be achieved when stepping is performed for more than 30 min, as noted earlier, using stricter controls for movement and when repeating this experiment using the newer generation of FosTRAP mice (DeNardo et al. 2019). It remains unclear as to what features of neuronal activity (e.g., firing rate, frequency, bursting) trigger and define immediate early gene activation and whether these features are similar for all cell phenotypes. Future studies researching what properties of neural activity elicit c-Fos and tdTomato expression will lead to more concrete physiological interpretations. This study did not combine TRAP activity with electrophysiology or stimulation like previous studies where TRAP was elicited by complex experiences (Allen et al. 2017; Cazzulino et al. 2016; DeNardo et al. 2019; Tasaka et al. 2018; Ye et al. 2016). Combining FosTRAP with fixed-body electrophysiology setups (Deliagina et al. 2012; Musienko et al. 2020; Zelenin et al. 2015, 2016) can provide complementary data that will lead to more concrete interpretations.

Future applications. The FosTRAP model provides a tool for visualizing the processes of activated neurons that would allow for characterizing the connectivity of spinal networks activated during different conditions. The value of these analyses can be enhanced with tissue-clearing techniques (Chung and Deisseroth 2013; Soderblom et al. 2015; Treweek et al. 2015; Yang et al. 2014) along with automated segmentation techniques (Pham et al. 2018). This technique can also potentially further characterize functional reorganization after traumatic effects (Courtine et al. 2009), rehabilitation (Fong et al. 2005; Ichiyama et al. 2008), or during development (Ohira et al. 2001; Sylos-Labini et al. 2020; Walton et al. 2005).

Conclusion. The present data are consistent with there being multiple functional parallel links among spinal networks that are activated when performing a highly repetitive motor task. Although this concept is well established (Côté et al. 2002; Latash 2012a, 2012b), this redundancy might have been assumed to be derived largely from the brain, but the present data suggest that a substantial level of redundancy is intrinsic to spinal networks. These observations also imply that each repetition of a motor event is defined probabilistically within and among spinal and supraspinal networks. This, in turn, results in activation of different subsets of neurons that form synergistic, coherent activations in space and time that is driven largely by proprioception and cutaneous input to the spinal neurons, similar to concepts proposed by Bizzi and colleagues (Cheung et al. 2005; d'Avella et al. 2003). Because of the limitations of the current work, these conclusions are not definitive. However, the results are compelling enough to warrant further investigation.

ACKNOWLEDGMENTS

We acknowledge all the students who have contributed to this study, especially Michael Thornton for assistance with CLARITY and staining with Chx10. Without the students' efforts, this study would not be possible. We also acknowledge the Advanced Light Microscopy/Spectroscopy Core at the California NanoSystems Institute at UCLA for the use of the confocal microscopes to acquire the CLARITY image stacks.

GRANTS

This imaging was made possible due to core vouchers from the UCLA Clinical and Translational Science Institute through National Institutes of Health Grant, UL1TR000124 as well as the Broccoli Foundation; Nanette and Burt Forester, Be13ve in Miracles Foundation; and PwC and Roberta Wilson for support of the whole study.

DISCLOSURES

V. R. Edgerton holds shareholder interest in NeuroRecoveryTechnologies and SpineX. V. R. Edgerton is also on the Scientific Advisory Board for SpineX and on the Board of Advisors for inVivoTherapeutics and ArianRF. V. R. Edgerton holds certain inventorship rights on intellectual property licensed by The Regents of the University of California to NeuroRecoveryTechnologies and its subsidiaries. No conflicts of interest, financial or otherwise, are declared by the authors.

AUTHOR CONTRIBUTIONS

B.N.P. and N.T. conceived and designed research; B.N.P., J.L., H.A., and H. Z. performed experiments; B.N.P., J.L., H.A., O.K., P.S., C.N., and S.G. analyzed data; B.N.P., N.T., J.L., A.G., and V.R.E., interpreted results of experiments; B.N.P., N.T., and J.L. prepared figures; B.N.P. drafted manuscript; B.N. P., N.T., A.G., and V.R.E., edited and revised manuscript; B.N.P. and V.R.E. approved final version of manuscript.

REFERENCES

Ahn SN, **Guu JJ**, **Tobin AJ**, **Edgerton VR**, **Tillakaratne NJ.** Use of c-fos to identify activity-dependent spinal neurons after stepping in intact adult rats. *Spinal Cord* 44: 547–559, 2006. doi:10.1038/sj.sc.3101862.

Allen WE, **DeNardo LA**, **Chen MZ**, **Liu CD**, **Loh KM**, **Fenno LE**, **Ramakrishnan C**, **Deisseroth K**, **Luo L.** Thirst-associated preoptic neurons encode an aversive motivational drive. *Science* 357: 1149–1155, 2017. doi:10.1126/science.aan6747.

Barajon I, **Gossard JP**, **Hultborn H.** Induction of fos expression by activity in the spinal rhythm generator for scratching. *Brain Res* 588: 168–172, 1992. doi:10.1016/0006-8993(92)91359-M.

Bellardita C, **Kiehn O.** Phenotypic characterization of speed-associated gait changes in mice reveals modular organization of locomotor networks. *Curr Biol* 25: 1426–1436, 2015. doi:10.1016/j.cub.2015.04.005.

Benedetti BL, **Glazewski S**, **Barth AL.** Reliable and precise neuronal firing during sensory plasticity in superficial layers of primary somatosensory cortex. *J Neurosci* 29: 11817–11827, 2009. doi:10.1523/JNEUROSCI.3431-09.2009.

Berkowitz A. Multifunctional and specialized spinal interneurons for turtle limb movements. *Ann N Y Acad Sci* 1198: 119–132, 2010. doi:10.1111/j.1749-6632.2009.05428.x.

Berkowitz A, **Roberts A**, **Soffe SR.** Roles for multifunctional and specialized spinal interneurons during motor pattern generation in tadpoles, zebrafish larvae, and turtles. *Front Behav Neurosci* 4: 36, 2010. doi:10.3389/fnbeh.2010.00036.

Bernshtein NA. *The Co-ordination and Regulation of Movements*. Oxford, New York: Pergamon Press, 1967.

Borowska J, **Jones CT**, **Zhang H**, **Blacklaws J**, **Goulding M**, **Zhang Y.** Functional subpopulations of V3 interneurons in the mature mouse spinal cord. *J Neurosci* 33: 18553–18565, 2013. doi:10.1523/JNEUROSCI.2005-13.2013.

Briggman KL, **Kristan WB Jr.** Multifunctional pattern-generating circuits. *Annu Rev Neurosci* 31: 271–294, 2008. doi:10.1146/annurev.neuro.31.060407.125552.

Caggiano V, **Cheung VC**, **Bizzi E.** An optogenetic demonstration of motor modularity in the mammalian spinal cord. *Sci Rep* 6: 35185, 2016. doi:10.1038/srep35185.

Cai LL, **Fong AJ**, **Otoshi CK**, **Liang Y**, **Burdick JW**, **Roy RR**, **Edgerton VR.** Implications of assist-as-needed robotic step training after a complete spinal cord injury on intrinsic strategies of motor learning. *J Neurosci* 26: 10564–10568, 2006. doi:10.1523/JNEUROSCI.2266-06.2006.

Cazzulino AS, **Martinez R**, **Tomm NK**, **Denny CA.** Improved specificity of hippocampal memory trace labeling. *Hippocampus* 26: 752–762, 2016. doi:10.1002/hipo.22556.

Chatzi C, **Zhang Y**, **Hendricks WD**, **Chen Y**, **Schnell E**, **Goodman RH**, **Westbrook GL.** Exercise-induced enhancement of synaptic function triggered by the inverse BAR protein, Mtss1L. *eLife* 8: e45920, 2019. doi:10.7554/eLife.45920.

Cheung VC, **d'Avella A**, **Tresch MC**, **Bizzi E.** Central and sensory contributions to the activation and organization of muscle synergies during natural motor behaviors. *J Neurosci* 25: 6419–6434, 2005. doi:10.1523/JNEUROSCI.4904-04.2005.

Chevalier C, **Nicolas JF**, **Petit AC.** Preparation and delivery of 4-hydroxy-tamoxifen for clonal and polyclonal labeling of cells of the surface ectoderm, skin, and hair follicle. *Methods Mol Biol* 1195: 239–245, 2014. doi:10.1007/7651_2013_63.

Chung K, **Deisseroth K.** CLARITY for mapping the nervous system. *Nat Methods* 10: 508–513, 2013 [Erratum in *Nat Methods* 10: 1035, 2013]. doi:10.1038/nmeth.2481.

Côté JN, **Mathieu PA**, **Levin MF**, **Feldman AG.** Movement reorganization to compensate for fatigue during sawing. *Exp Brain Res* 146: 394–398, 2002. doi:10.1007/s00221-002-1186-6.

Courtine G, **Gerasimenko Y**, **van den Brand R**, **Yew A**, **Musienko P**, **Zhong H**, **Song B**, **Ao Y**, **Ichiyama RM**, **Lavrov I**, **Roy RR**, **Sofroniew MV**, **Edgerton VR.** Transformation of nonfunctional spinal circuits into functional states after the loss of brain input. *Nat Neurosci* 12: 1333–1342, 2009. doi:10.1038/nn.2401.

Courtine G, **Song B**, **Roy RR**, **Zhong H**, **Herrmann JE**, **Ao Y**, **Qi J**, **Edgerton VR**, **Sofroniew MV.** Recovery of supraspinal control of stepping via indirect propriospinal relay connections after spinal cord injury. *Nat Med* 14: 69–74, 2008. doi:10.1038/nm1682.

d'Avella A, **Saltiel P**, **Bizzi E.** Combinations of muscle synergies in the construction of a natural motor behavior. *Nat Neurosci* 6: 300–308, 2003. doi:10.1038/nn1010.

Dai X, **Noga BR**, **Douglas JR**, **Jordan LM.** Localization of spinal neurons activated during locomotion using the c-fos immunohistochemical method. *J Neurophysiol* 93: 3442–3452, 2005. doi:10.1152/jn.00578.2004.

Dale EA, **Ng M**, **Zhong H**, **Roy RR**, **Tillakaratne NJK**, **Edgerton VR**, **Kim JA.** Characterization of spinal interneurons responsible for stepping in spinally transected mice (Abstract). Program No. 732.06. 2014 Neuroscience Meeting Planner. Washington, DC, November 15–19, 2014.

De Leon RD, **Hodgson JA**, **Roy RR**, **Edgerton VR.** Full weight-bearing hindlimb standing following stand training in the adult spinal cat. *J Neurophysiol* 80: 83–91, 1998. doi:10.1152/jn.1998.80.1.83.

De Leon RD, **Hodgson JA**, **Roy RR**, **Edgerton VR.** Retention of hindlimb stepping ability in adult spinal cats after the cessation of step training. *J Neurophysiol* 81: 85–94, 1999. doi:10.1152/jn.1999.81.1.85.

Deliagina TG, **Zelenin PV**, **Orlovsky GN.** Physiological and circuit mechanisms of postural control. *Curr Opin Neurobiol* 22: 646–652, 2012. doi:10.1016/j.conb.2012.03.002.

DeNardo LA, **Liu CD**, **Allen WE**, **Adams EL**, **Friedmann D**, **Fu L**, **Guenthner CJ**, **Tessier-Lavigne M**, **Luo L.** Temporal evolution of cortical ensembles promoting remote memory retrieval. *Nat Neurosci* 22: 460–469, 2019. doi:10.1038/s41593-018-0318-7.

Esposito MS, **Capelli P**, **Arber S.** Brainstem nucleus MdV mediates skilled forelimb motor tasks. *Nature* 508: 351–356, 2014. doi:10.1038/nature13023.

Fong AJ, **Cai LL**, **Otoshi CK**, **Reinkensmeyer DJ**, **Burdick JW**, **Roy RR**, **Edgerton VR.** Spinal cord-transected mice learn to step in response to quipazine treatment and robotic training. *J Neurosci* 25: 11738–11747, 2005. doi:10.1523/JNEUROSCI.1523-05.2005.

Gao YJ, **Ji RR.** c-Fos and pERK, which is a better marker for neuronal activation and central sensitization after noxious stimulation and tissue injury? *Open Pain J* 2: 11–17, 2009. doi:10.2174/1876386300902010011.

Gerasimenko Y, **Sayenko D**, **Gad P**, **Liu CT**, **Tillakaratne NJK**, **Roy RR**, **Kozlovskaya I**, **Edgerton VR.** Feed-forwardness of spinal networks in posture and locomotion. *Neuroscientist* 23: 441–453, 2017. doi:10.1177/1073858416683681.

Girasole AE, **Lum MY**, **Nathaniel D**, **Bair-Marshall CJ**, **Guenthner CJ**, **Luo L**, **Kreitzer AC**, **Nelson AB.** A subpopulation of striatal neurons mediates levodopa-induced dyskinesia. *Neuron* 97: 787–795.e6, 2018. doi:10.1016/j.neuron.2018.01.017.

Groves A, **Kihara Y**, **Jonnalagadda D**, **Rivera R**, **Kennedy G**, **Mayford M**, **Chun J.** A functionally defined *in vivo* astrocyte population identified by c-Fos activation in a mouse model of multiple sclerosis modulated by S1P signaling: immediate-early astrocytes (*ieAstrocytes*). *eNeuro* 5: ENEURO.0239-18.2018, 2018. doi:10.1523/ENEURO.0239-18.2018.

Guenthner CJ, **Miyamichi K**, **Yang HH**, **Heller HC**, **Luo L.** Permanent genetic access to transiently active neurons via TRAP: targeted recombination in active populations. *Neuron* 78: 773–784, 2013 [Erratum in *Neuron* 79: 1257, 2013]. doi:10.1016/j.neuron.2013.03.025.

Haar S, **Donchin O**, **Dinstein I.** Individual movement variability magnitudes are explained by cortical neural variability. *J Neurosci* 37: 9076–9085, 2017. doi:10.1523/JNEUROSCI.1650-17.2017.

Hao ZZ, **Berkowitz A.** Shared components of rhythm generation for locomotion and scratching exist prior to motoneurons. *Front Neural Circuits* 11: 54, 2017. doi:10.3389/fncir.2017.00054.

Huang A, **Noga BR**, **Carr PA**, **Fedirchuk B**, **Jordan LM.** Spinal cholinergic neurons activated during locomotion: localization and electrophysiological

characterization. *J Neurophysiol* 83: 3537–3547, 2000. doi:10.1152/jn.2000.83.6.3537.

Hunt SP, **Pini A**, **Evan G.** Induction of c-fos-like protein in spinal cord neurons following sensory stimulation. *Nature* 328: 632–634, 1987. doi:10.1038/328632a0.

Ichiyama RM, **Courtine G**, **Gerasimenko YP**, **Yang GJ**, **van den Brand R**, **Lavrov IA**, **Zhong H**, **Roy RR**, **Edgerton VR.** Step training reinforces specific spinal locomotor circuitry in adult spinal rats. *J Neurosci* 28: 7370–7375, 2008. doi:10.1523/JNEUROSCI.1881-08.2008.

Ivanenko YP, **Cappellini G**, **Solopova IA**, **Grishin AA**, **Maclellan MJ**, **Poppele RE**, **Lacquaniti F.** Plasticity and modular control of locomotor patterns in neurological disorders with motor deficits. *Front Comput Neurosci* 7: 123, 2013. doi:10.3389/fncom.2013.00123.

Jankowska E. Spinal interneuronal systems: identification, multifunctional character and reconfigurations in mammals. *J Physiol* 533: 31–40, 2001. doi:10.1111/j.1469-7793.2001.0031b.x.

Joshi RS, **Panicker MM.** Identifying the *In Vivo* cellular correlates of antipsychotic drugs. *eNeuro* 5: ENEURO.0220-18.2018, 2018. doi:10.1523/ENEURO.0220-18.2018.

Kim JA, **Xiao MS**, **Hornak AJ**, **Mikhaeil M**, **Esquivel V**, **Gonzalez EJ**, **Duru P**, **Joseph MS**, **Zhong H**, **Roy RR**, **Edgerton VR**, **Tillakaratne NJK.** Activated spinal neurons during quadrupedal stepping in adult intact mice injected with pseudorabies virus into the tibialis anterior (Abstract). Program No. 832.04. 2013 Neuroscience Meeting Planner. San Diego, CA, November 9–13, 2013.

Latash ML. The bliss (not the problem) of motor abundance (not redundancy). *Exp Brain Res* 217: 1–5, 2012a. doi:10.1007/s00221-012-3000-4.

Latash ML. Movements that are both variable and optimal. *J Hum Kinet* 34: 5–13, 2012b. doi:10.2478/v10078-012-0058-9.

Latash ML, **Zatsiorsky VM.** *Biomechanics and Motor Control: Defining Central Concepts*. London, UK: Elsevier/AP, 2016.

Lavrov I, **Courtine G**, **Dy CJ**, **van den Brand R**, **Fong AJ**, **Gerasimenko Y**, **Zhong H**, **Roy RR**, **Edgerton VR.** Facilitation of stepping with epidural stimulation in spinal rats: role of sensory input. *J Neurosci* 28: 7774–7780, 2008. doi:10.1523/JNEUROSCI.1069-08.2008.

Levine AJ, **Hinckley CA**, **Hilde KL**, **Driscoll SP**, **Poon TH**, **Montgomery JM**, **Pfaff SL.** Identification of a cellular node for motor control pathways. *Nat Neurosci* 17: 586–593, 2014. doi:10.1038/nn.3675.

Li N, **Daie K**, **Svoboda K**, **Druckmann S.** Robust neuronal dynamics in premotor cortex during motor planning. *Nature* 532: 459–464, 2016 [Erratum in *Nature* 537: 122, 2016]. doi:10.1038/nature17643.

Lisberger SG, **Medina JF.** How and why neural and motor variation are related. *Curr Opin Neurobiol* 33: 110–116, 2015. doi:10.1016/j.conb.2015.03.008.

Loy DN, **Magnuson DS**, **Zhang YP**, **Onifer SM**, **Mills MD**, **Cao QL**, **Darnall JB**, **Fajardo LC**, **Burke DA**, **Whittemore SR.** Functional redundancy of ventral spinal locomotor pathways. *J Neurosci* 22: 315–323, 2002. doi:10.1523/JNEUROSCI.22-01-00315.2002.

Marder E, **Goaillard JM.** Variability, compensation and homeostasis in neuron and network function. *Nat Rev Neurosci* 7: 563–574, 2006. doi:10.1038/nrn1949.

McLean DL, **Masino MA**, **Koh IY**, **Lindquist WB**, **Fetcho JR.** Continuous shifts in the active set of spinal interneurons during changes in locomotor speed. *Nat Neurosci* 11: 1419–1429, 2008. doi:10.1038/nn.2225.

Miller JE, **Hilliard AT**, **White SA.** Song practice promotes acute vocal variability at a key stage of sensorimotor learning. *PLoS One* 5: e8592, 2010. doi:10.1371/journal.pone.0008592.

Muir DA, **Compston DA.** Growth factor stimulation triggers apoptotic cell death in mature oligodendrocytes. *J Neurosci Res* 44: 1–11, 1996. doi:3.0.CO;2-L">10.1002/(SICI)1097-4547(19960401)44:1<1:AID-JNR1>3.0.CO;2-L.

Musienko P, **Courtine G**, **Tibbs JE**, **Kilimnik V**, **Savochin A**, **Garfinkel A**, **Roy RR**, **Edgerton VR**, **Gerasimenko Y.** Somatosensory control of balance during locomotion in decerebrated cat. *J Neurophysiol* 107: 2072–2082, 2012. doi:10.1152/jn.00730.2011.

Musienko PE, **Lyalka VF**, **Gorskii OV**, **Merkulyeva N**, **Gerasimenko YP**, **Deliagina TG**, **Zelenin PV.** Comparison of operation of spinal locomotor networks activated by supraspinal commands and by epidural stimulation of the spinal cord in cats. *J Physiol* 598: 3459–3483, 2020. doi:10.1113/JP279460.

Ohira Y, **Tanaka T**, **Yoshinaga T**, **Kawano F**, **Nomura T**, **Nonaka I**, **Allen DL**, **Roy RR**, **Edgerton VR.** Ontogenetic, gravity-dependent development of rat soleus muscle. *Am J Physiol Cell Physiol* 280: C1008–C1016, 2001. doi:10.1152/ajpcell.2001.280.4.C1008.

Pham B, **Gaonkar B**, **Whitehead W**, **Moran S**, **Dai Q**, **Macyszyn L**, **Edgerton VR.** Cell counting and segmentation of immunohistochemical images in the spinal cord: comparing deep learning and traditional approaches. *Annu Int Conf IEEE Eng Med Biol Soc* 2018: 842–845, 2018. doi:10.1109/EMBC.2018.8512442.

Saltiel P, **Wyler-Duda K**, **d'Avella A**, **Ajemian RJ**, **Bizzi E.** Localization and connectivity in spinal interneuronal networks: the adduction-caudal extension-flexion rhythm in the frog. *J Neurophysiol* 94: 2120–2138, 2005. doi:10.1152/jn.00117.2005.

Sauerbrei BA, **Lubenov EV**, **Siapas AG.** Structured variability in Purkinje cell activity during locomotion. *Neuron* 87: 840–852, 2015. doi:10.1016/j.neuron.2015.08.003.

Shah PK, **Gerasimenko Y**, **Shyu A**, **Lavrov I**, **Zhong H**, **Roy RR**, **Edgerton VR.** Variability in step training enhances locomotor recovery after a spinal cord injury. *Eur J Neurosci* 36: 2054–2062, 2012. doi:10.1111/j.1460-9568.2012.08106.x.

Shenoy KV, **Sahani M**, **Churchland MM.** Cortical control of arm movements: a dynamical systems perspective. *Annu Rev Neurosci* 36: 337–359, 2013. doi:10.1146/annurev-neuro-062111-150509.

So K, **Ganguly K**, **Jimenez J**, **Gastpar MC**, **Carmena JM.** Redundant information encoding in primary motor cortex during natural and prosthetic motor control. *J Comput Neurosci* 32: 555–561, 2012. doi:10.1007/s10827-011-0369-1.

Soderblom C, **Lee DH**, **Dawood A**, **Carballosa M**, **Santamaria AJ**, **Benavides FD**, **Jergova S**, **Grumbles RM**, **Thomas CK**, **Park KK**, **Guest JD**, **Lemmon VP**, **Lee JK**, **Tsoulfas P.** 3D imaging of axons in transparent spinal cords from rodents and nonhuman primates. *eNeuro* 2: ENEURO.0001-15.2015, 2015. doi:10.1523/ENEURO.0001-15.2015.

Sylos-Labini F, **La Scaleia V**, **Cappellini G**, **Fabiano A**, **Picone S**, **Keshishian ES**, **Zhvansky DS**, **Paolillo P**, **Solopova IA**, **d'Avella A**, **Ivanenko Y**, **Lacquaniti F.** Distinct locomotor precursors in newborn babies. *Proc Natl Acad Sci USA* 117: 9604–9612, 2020. doi:10.1073/pnas.1920984117.

Tasaka GI, **Guenthner CJ**, **Shalev A**, **Gilday O**, **Luo L**, **Mizrahi A.** Genetic tagging of active neurons in auditory cortex reveals maternal plasticity of coding ultrasonic vocalizations. *Nat Commun* 9: 871, 2018. doi:10.1038/s41467-018-03183-2.

Tillakaratne NJ, **Duru P**, **Fujino H**, **Zhong H**, **Xiao MS**, **Edgerton VR**, **Roy RR.** Identification of interneurons activated at different inclines during treadmill locomotion in adult rats. *J Neurosci Res* 92: 1714–1722, 2014. doi:10.1002/jnr.23437.

Treweek JB, **Chan KY**, **Flytzanis NC**, **Yang B**, **Deverman BE**, **Greenbaum A**, **Lignell A**, **Xiao C**, **Cai L**, **Ladinsky MS**, **Bjorkman PJ**, **Fowlkes CC**, **Gradinaru V.** Whole-body tissue stabilization and selective extractions via tissue-hydrogel hybrids for high-resolution intact circuit mapping and phenotyping. *Nat Protoc* 10: 1860–1896, 2015. doi:10.1038/nprot.2015.122.

Walton KD, **Harding S**, **Anschel D**, **Harris YT**, **Llinás R.** The effects of microgravity on the development of surface righting in rats. *J Physiol* 565: 593–608, 2005. doi:10.1113/jphysiol.2004.074385.

Watson C, **Paxinos G**, **Kayalioglu G.** *The Spinal Cord*. London, UK: Academic Press, 2009.

Yang B, **Treweek JB**, **Kulkarni RP**, **Deverman BE**, **Chen CK**, **Lubeck E**, **Shah S**, **Cai L**, **Gradinaru V.** Single-cell phenotyping within transparent intact tissue through whole-body clearing. *Cell* 158: 945–958, 2014. doi:10.1016/j.cell.2014.07.017.

Ye L, **Allen WE**, **Thompson KR**, **Tian Q**, **Hsueh B**, **Ramakrishnan C**, **Wang AC**, **Jennings JH**, **Adhikari A**, **Halpern CH**, **Witten IB**, **Barth AL**, **Luo L**, **McNab JA**, **Deisseroth K.** Wiring and molecular features of prefrontal ensembles representing distinct experiences. *Cell* 165: 1776–1788, 2016. doi:10.1016/j.cell.2016.05.010.

Zelenin PV, **Hsu LJ**, **Lyalka VF**, **Orlovsky GN**, **Deliagina TG.** Putative spinal interneurons mediating postural limb reflexes provide a basis for postural control in different planes. *Eur J Neurosci* 41: 168–181, 2015. doi:10.1111/ejn.12780.

Zelenin PV, **Lyalka VF**, **Orlovsky GN**, **Deliagina TG.** Effect of acute lateral hemisection of the spinal cord on spinal neurons of postural networks. *Neuroscience* 339: 235–253, 2016. doi:10.1016/j.neuroscience.2016.09.043.

Ziegler MD, **Zhong H**, **Roy RR**, **Edgerton VR.** Why variability facilitates spinal learning. *J Neurosci* 30: 10720–10726, 2010. doi:10.1523/JNEUROSCI.1938-10.2010.